Electronic Supplementary Material (ESI) for Journal of Materials Chemistry C.

Supporting information

An illustrative understanding on strengthening in stability and efficiency of perovskite solar cells: Utilization of the perovskite-constructed polymer hybrid system of PHQACl-CN inclusion

Providence Buregeya Ingabire[a], Ningxia Gu [a], Ning Lei [a], Lixin Song[a,*], Xiang Chen[a],Pengyun Zhang[a], Shouwen Chen[b], Pingfan Du[a], Jie Xiong[a*]

[a]. *College of Textile Science and Engineering, Zhejiang Sci-Tech University, Hangzhou, 310018, China*

[b]. *School of Environmental and Biological Engineering*, *Nanjing University of Science & Technology, Nanjing 210094, China*

*Corresponding author Tex: +86 571 86843586; E-mail address: lxsong12@zstu.edu.cn; jxiong@zstu.edu.cn

Experimental section

Materials: Lead iodide (PbI_2, 99.99%), methylammonium iodide (MAI, >99.5%), and $PC_{61}BM$ are supplied by Xi'an Polymer Light Technology Corp. Fluorine-doped tin oxide (FTO, 14 Ω sq^{-1}) substrates are provided by Advanced Election Technology Co., Ltd. Anhydrous dimethyl sulfoxide (DMSO, 99.7%), isopropanol (IPA, 99.7%), anhydrous dimethylformamide (DMF, 99.8%), anhydrous ethanol (99.7%), acetone (99%), anhydrous chlorobenzene (CB, 99.8%), anhydrous ethyl acetate (EA, 99.5%) are all obtained from either Sigma-Aldrich or Shanghai Aladdin Biochemical Technology Co., Ltd. Prior to the polymerization, 2,2'-Bis(4-hydroxyphenyl) hexafluoropropane (HFBPA) and 4,4'-(9-fluorenylidene) diphenol (BHPF) are both recrystallized from water/ethanol mixture. Toluene is distilled after phosphorus pentoxide dehydration and stored over 4Å molecular sieves. Anhydrous carbonate potassium (K_2CO_3) is dried at 120 °C for 24 h in *vacuo* before use. N, N-Dimethylacetamide (DMAc) is stirred over CaH_2 for 24 h, then distilled under reduced pressure and stored over 4Å molecular sieves. Melamine, 1,1',2,2'-tetrachloroethane (TCE), chlorodimethyl ether (CME), stannic chloride ($SnCl_4$), N,N'-dimethylformamide (DMF), concentrated sulfuric acid (98 wt%), ethanol, trimethylamine (TMA, 33 wt% in water) and other reagents are supplied by commercial sources and utilized without purification.

Material Characterization:

Fourier transform infrared (FTIR) spectra are recorded using Nicolet 5700 Fourier Transform Infrared Spectrometer. X-ray diffraction pattern (XRD, Thermo Fisher Scientific) is evaluated with Cu Kα radiation using in an angle range and scan rate of 5-40° and 3°/min, respectively. Scanning electron microscopy (SEM) images of top-view and cross-sectional samples and energy dispersive X-ray spectroscopy (EDS) measurement are obtained using a scanning electron microscope (Zeiss SUPRA 55) with an electron beam accelerated voltage at 3 kV, enabling operation at a variety of currents. With the Ultraviolet and visible spectrophotometry (UV-vis, P4, China), the light absorption spectra of the perovskite films are recorded. The steady-state photoluminescence (PL) spectrum is tested by Fluo Time 300 fluorophotometer Lifetime Spectrometer with an excitation wavelength of 520 nm. Time-

resolved PL (TRPL) decay is carried out using a picosecond diode laser with an excitation wavelength of 780 nm. The electrochemical impedance spectroscopy (EIS) is evaluated by a potentiostat (Im6ex/Zahner) to examine charge transfer properties and battery performance with an alternative signal amplitude of 10 mV and a frequency range of 0.01-100 kHz. The contact angle measurement instrument (Fangrui, Shanghai) is employed to record the contact angle of water droplets on top-view of perovskite film. Thermogravimetric analysis (TGA, China) is measured under nitrogen atmosphere. The current density versus voltage (J-V) curves of the fabricated device structures are collected by a Keithley 2400 Sourcemeter with a solar simulator (USA) under 100 mW cm^{-2} illumination (AM 1.5 G irradiation). To confirm data about the resonance from protons adjacent to carbon, we have performed 1-Hydrogen nuclear magnetic resonance (^{1}H NMR) spectra using a Bruker 510 spectrophotometer (500 MHz) with deuterated dimethylsulfoxide (DMSO-d6) or chloroform (CDCl3) solution at room temperature using tetramethylsilane internal reference. The molecular weights of the synthesized polymers are collected using gel permeation chromatography (GPC) using an HPLC system (Dionex Ultimate 3000) equipped with a PLgel columns (Agilent) eluted with DMF (containing 0.05% LiBr) at a flow rate of 1.0 mL/min based on the calibration curve of polystyrene standards.

Polymerization process

The polymer has been prepared by nucleophilic substitution, as detailed in the literatures [1, 2] and its synthetic route in Scheme S1.

Synthesis of poly(aryl ether sulfone)s Chloromethylated Polymer (CHLMP)

To a 100 mL dried three-necked flask equipped with a nitrogen inlet/outlet, condenser, and mechanical stirrer, 1.0 g polymer fibers are initially dissolved in 15 mL of TCE in at 65 ^oC to obtain a homogeneous solution. The solution in flask is fixed in an ice-water bath and then the mixture of 5 mL TCE, 4.92 mL CME and 0.15 mL stannic chloride is dropwisely added to the solution with stirring at 30 ^oC for 24 h. After precipitating the resultant solution into in ethanol, the polymer product is washed with ethanol again before being dried at 65 ^oC under vacuum for 7 h. The synthesized CHLMP products are 92-95% in yield.

Synthesis of Polymer of Quaternary Ammonium Chloride (PQACl)

Prior to quaternization procedure, 0.8 g CHLMP products are dissolved in 16 mL of DMAc in a 100 mL three-necked flask. After that, 1.5 mL trimethylamine (TMA) aqueous solution is added to the mixture with a mechanically stirring at room temperature for 36 h to integrate quaternary ammonium groups. After being poured into IPA, the collected polymers are washed with deionized water before being dried at 65 °C under vacuum for 7 h. The synthesized PQACl products are 88-91% in yield

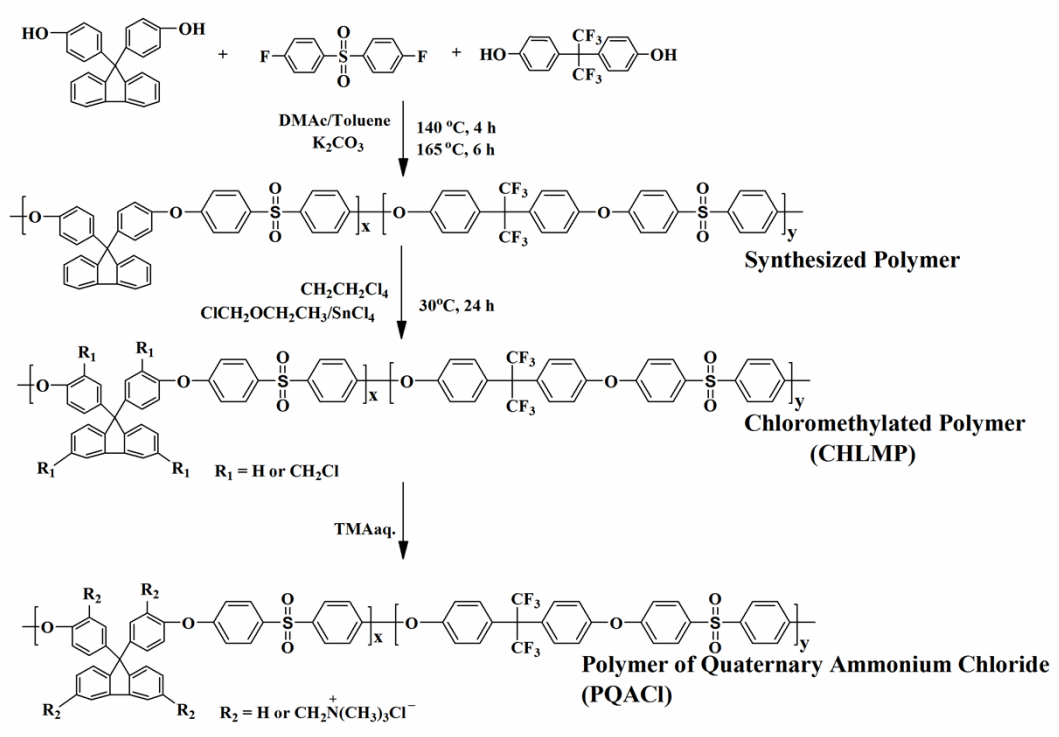

Scheme 1. Synthetic process of PQACl

Synthesis of Bulk Graphitic Carbon Nitride (bC_3N_4) and sC_3N_4 nanosheets

An appropriate amount of bC_3N_4 is prepared by placing 8 g melamine in an alumina crucible, then covering and positioning them suitably in a muffle furnace [3, 4] and the heating treatment is performed at 550 °C for 4 h with a heating/cooling rate of 3 °C/min. The obtained yellow-colored powder is processed by grounding with blender into fine particulate powder, named as bC_3N_4. To a 250 mL conical flask equipped with a mechanical stirrer, 5 g bC_3N_4 is added to 100 mL concentrated sulfuric acid with heating at 100 °C for 3 h to make a uniform mixture, which is slowly changed to pale-yellow solution. By conducting an experiment in the fume-hood, after cooling the flask containing bC_3N_4 particulate solution in an ice-bath, the

addition of 800 mL deionized water gradually leads to the change in color of mixture from yellow to white, indicating the exfoliation and deformation processes induced by concentrated sulfuric acid approach [5, 6]. To collect the sC_3N_4 nanosheets (the C_3N_4 nanosheets derived from sulfuric acid treatment), the white precipitate materials are obtained by centrifugation at 4000 rpm for 10 minutes and washed with deionized water until neutral pH and heated at 60 °C for 24 h in a vacuum. These formed sC_3N_4 nanosheets are 14-16% in yield.

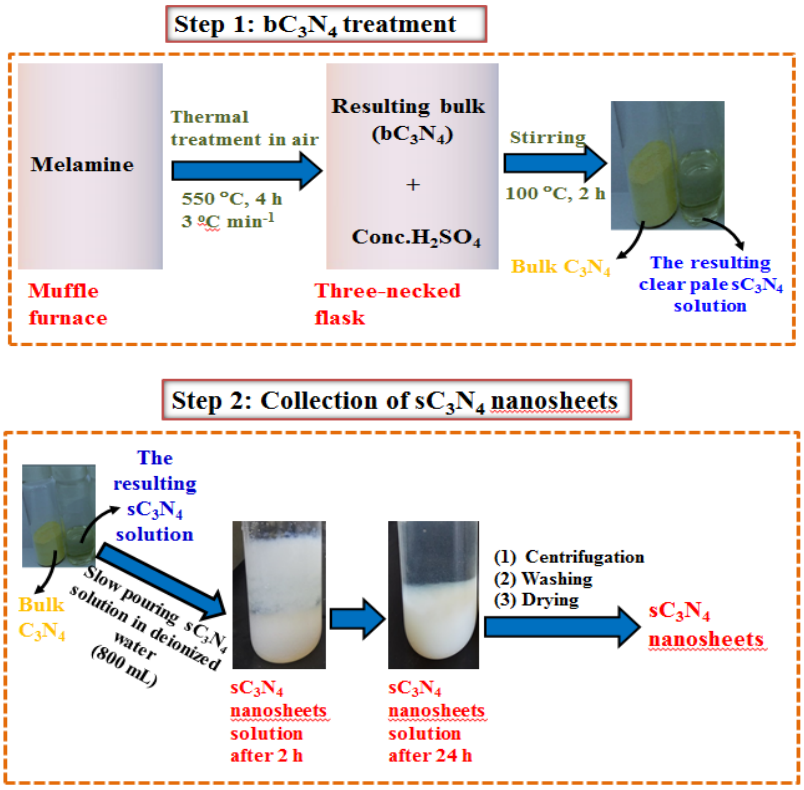

Scheme 2. Illustration of the synthesis of sC_3N_4 materials for use in perovskite films

Preparation of polymeric hybrid precursor solution (PHQACl-CN)

The polymeric solution is obtained by dissolving PQACl in DMF/DMSO (7.6:1) to form a 6 wt% solution at ambient temperature for 24 h and then the mixture is filtrated through a plug of cotton. To improve the polymer properties, aiming at their further applications; a small amount of sC_3N_4 is dispersed in 2 mL DMF/DMSO (7.6:1, v/v) with a mechanical stirring and ultrasonic treatment for 20 h at ambient temperature. After that, the resulting sC_3N_4 solution is properly added in the prepared polymeric solution with an ultrasonically mechanical stirring for 36 h. The resulting solution is noted as PQACl/sC_3N_4-x, where x denotes the weight percentage of the nanofillers to PQACl materials. In consideration of the promising traits, such as good solubility

(Table S1) and optimistic chemical structures of the formed polymer (Figure S1), together good thermal stability (Figure S2) and morphology (Figure S3); the existence of functional groups sites of sC_3N_4 materials (Scheme 3) within the synthesized polymer can provide additional benefits. Hence, PQACl/sC_3N_4-0.8 Polymer Hybrid solution (designated as PHQACl-CN) is selected as a precursor solution for constructing the polymer hybrid-based perovskite with PHQACl-CN due to the above mentioned good features of these components. From this perspective, PHQACl-CN is undoubtedly regarded as promising potential component about manufacturing high quality films in PSCs applications.

Preparation of polymeric precursor solution (PQACl) for perovskite film formation

In this investigation, PQACl polymer solutions are prepared by diluting 1.0 mL of the prepared PQACl precursor solution (6 wt% PQACl solution) to a final volume of 1.6 mL, 2.4 mL, 3.2 mL, 4.0 mL, and 6.4 mL with DMF/DMSO solvents mixture (7.6:1, v/v), and the resulting PQACl polymer solutions are denoted as PQACl1, PQACl2, PQACl3, PQACl4, and PQACl5, respectively. The prepared PQACl are subsequently constrained to stirring process at 60 ^oC for 6 h with ultrasonication treatment every 2 h, prior to use, in the formation of perovskite thin films.

Preparation of nanofiller precursor solution (sCN) for perovskite film formation

The sC_3N_4 precursor is dispersed in DMF/DMSO (7.6:1, v/v) at 3.5 mg/mL by an alternation of stirring and ultrasonication treatments. sCN materials solutions are prepared by diluting 1.0 mL of the processed sC_3N_4 precursor solution to a final volume of 1.6 mL, 2.4 mL, 3.2 mL, 4.0 mL, and 6.4 mL with DMF/DMSO solvents mixture (7.6:1, v/v), and the resulting materials solutions are denoted as sCN1, sCN2, sCN3, sCN4, and sCN5, respectively.

Preparation of different solutions of PHQACl-CN for perovskite film formation

To prepare various solutions of PHQACl-CN, we need to dilute 1.0 mL of the prepared PHQACl-CN precursor solution to a final volume of 1.6 mL, 2.4 mL, 3.2 mL, 4.0 mL and 6.4 with DMF/DMSO solvents mixture (7.6:1, v/v), and the emerging polymer hybrid solutions are appointed as PHQACl-CN1, PHQACl-CN2, PHQACl-CN3 and PHQACl-CN4, respectively. The obtained PHQACl-CN solutions are subsequently constrained to stirring process at 70 ^oC for

6 h with ultrasonication treatment every 2 h, prior to use, in the development of perovskite thin films.

Chemical structures of the synthesized polymeric materials (PQACl)

Figure S1 (a) and (b) provides the ^{1}H NMR spectra of CHLMP and PQACl, respectively. The peak located at 4.53 ppm corresponds to the chloromethylated groups on the polymer backbone, as indicated in Figure S1 (a). Newly formed peaks are at 2.97 ppm and 4.58 ppm matching with the protons in $N(CH_3)_3$ and CH_2N groups, respectively, proving the successful formation of the quaternized polymers, as illustrated in Figure S1(b).

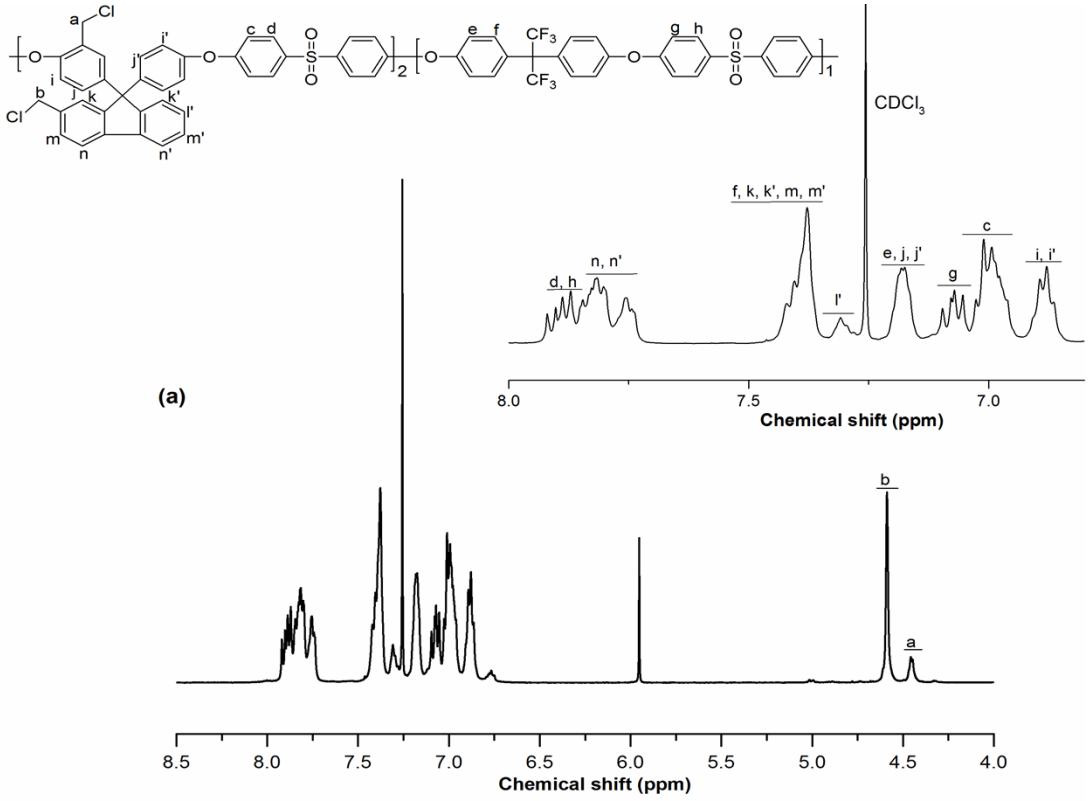

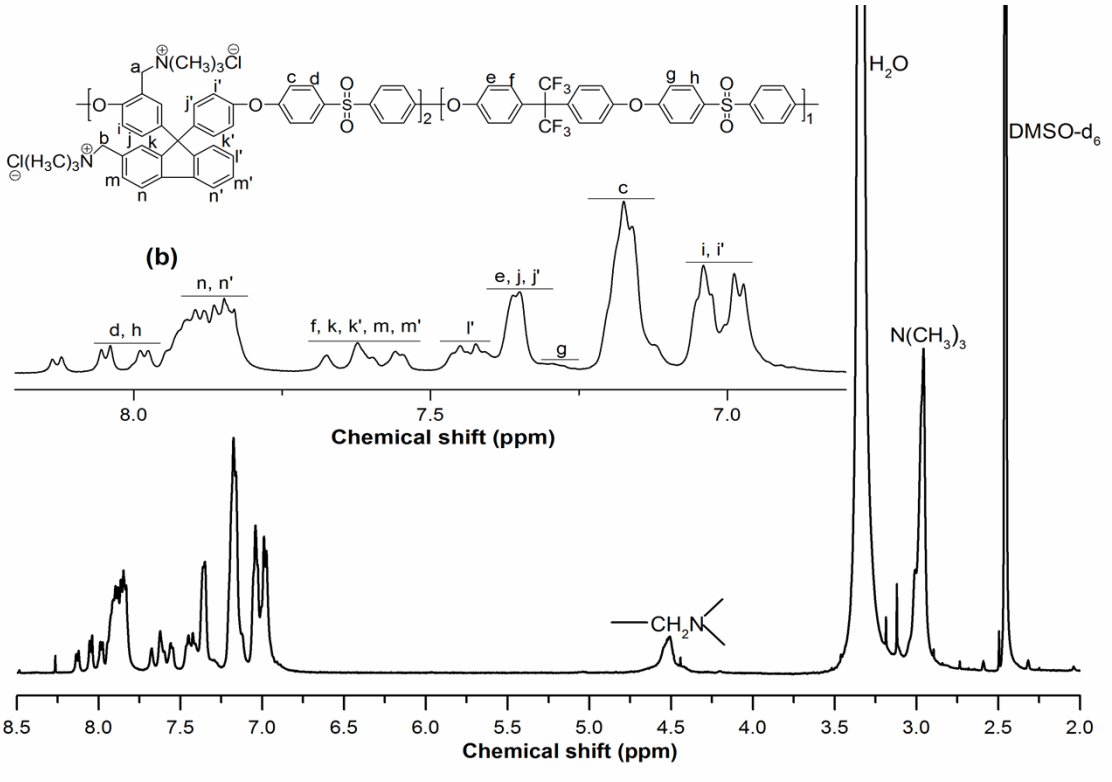

Figure S1. [1]H NMR spectra of a) CHLMP and b) PQACl

Thermal stability of films from developed PQACl polymer

As can been in Figure S2, the PQACl materials can satisfy the performance, stability and durability of photovoltaic equipment, revealing its suitability to the fabrication of respectable perovskite films.

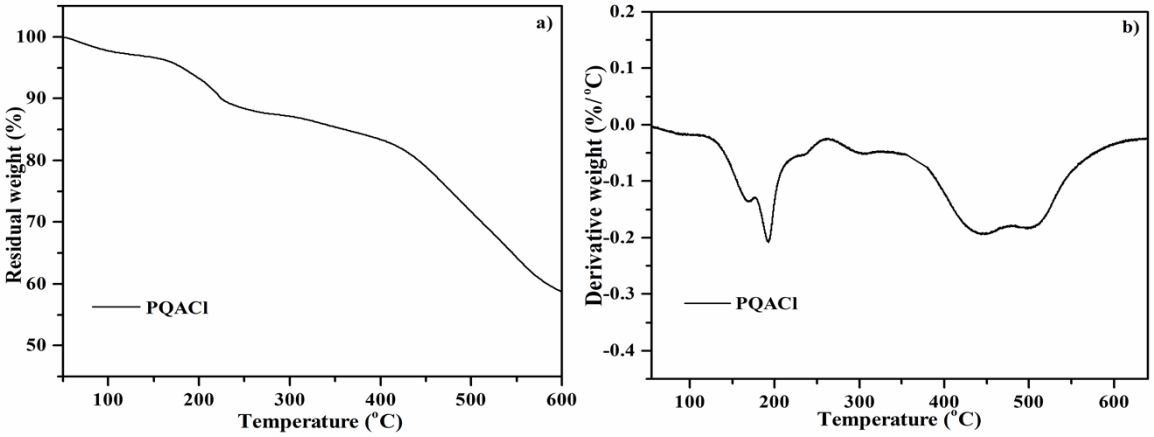

Figure S2. a)TGA and b) DTG of PQACl.

The three-step thermal degradation steps in the films (TGA & DTG) are:

- 1st step: The evaporation of water (below 120 °C);
- 2nd step: The degradation of quaternary ammonium groups (170-330 °C);
- 3rd step: The degradation of polymer backbones (above 400 °C).

Morphology of PQACl and PQACl/sC_3N_4

The change in the morphology is examined before employing the polymer hybrid materials in PSC device manipulation, as shown in Figure S3. Various amounts of sC_3N_4 (0.4; 0.8; 1.6) are dispersed in 2 mL DMF/DMSO (7.6:1, v/v) with a mechanical stirring and ultrasonic treatment for 20 h at ambient temperature. After that, the resulting sC_3N_4 solution is properly added in the prepared polymeric solution (6 wt% PQACl solution) with an ultrasonically mechanical stirring for 36 h. The resulting solution is poured onto a clean flat petri-dish and its drying treatment is carried out in a convection oven at 60 ^oC for 24 h to fabricate polymeric films, noted as PQACl/sC_3N_4-x, where x denotes the weight percentage of the nanofillers to PQACl materials. In consideration of the top-view morphology, PQACl/sC_3N_4-0.8 is the most efficient polymer hybrid.

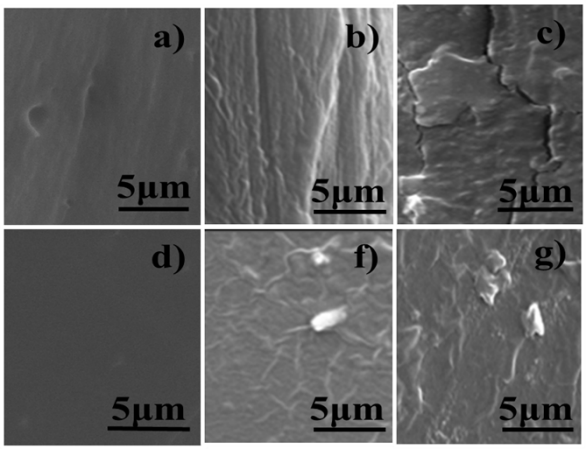

Figure S3. The surface and cross-sectional SEM images of the polymeric films from pure PQACl, PQACl/sC_3N_4-0.8, and PQACl/sC_3N_4-1.6.

FTIR of films from PQACl and PQACl/sC_3N_4

According to the results shown in Figure S4, the FTIR spectra of PQACl and PQACl/sC_3N_4 polymer treated with sC_3N_4 are similar. The peaks at 1581 cm^{-1} and 1480 cm^{-1} are ascribed to the existence of the skeletal vibrations of polymer backbone. The noticeable peak at 1242 cm^{-1} is assigned to the asymmetric vibration of the ether linkage and the peaks at 1292 cm^{-1} and 1150 cm^{-1} are allocated to the stretching vibrations of O=S=O. The peaks at 1630 cm^{-1} and 1375 cm^{-1} belong to the N-C and N-H groups of the quaternized polymer.

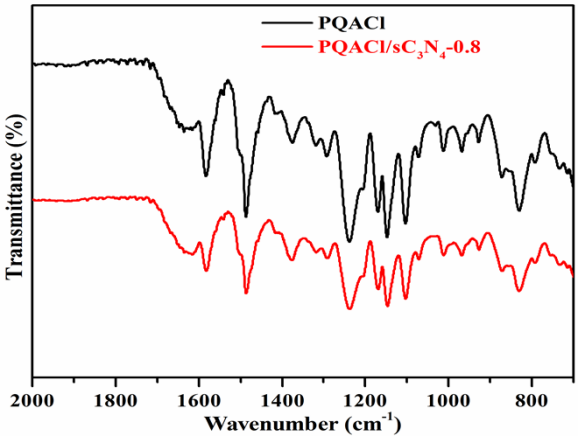

Figure S4. FTIR spectra of PQACl and PQACl/sC_3N_4.

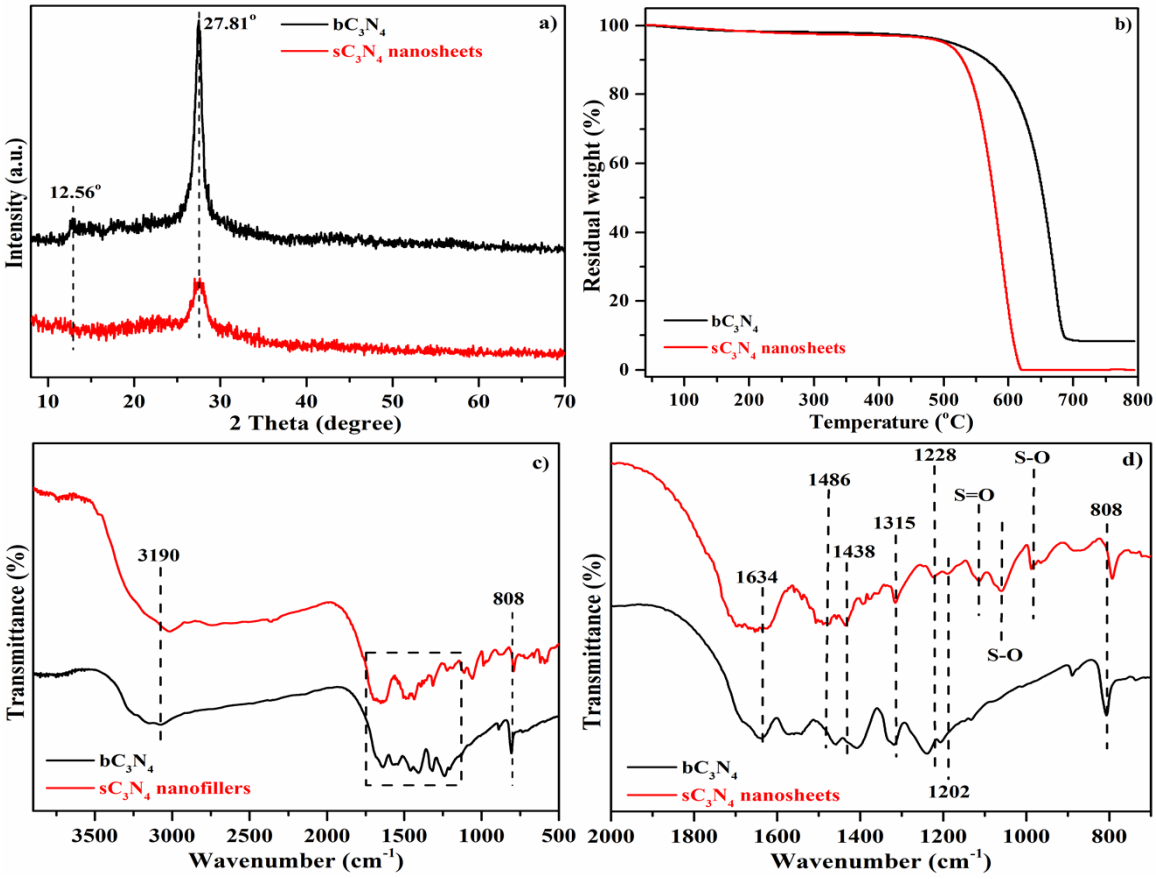

Figure S5. a) XRD, b) TGA, c) & d) FTIR of the bC_3N_4 & sC_3N_4

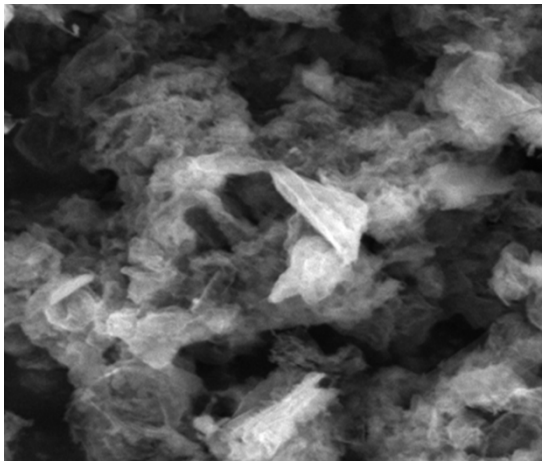

Figure S6. SEM image of sC_3N_4

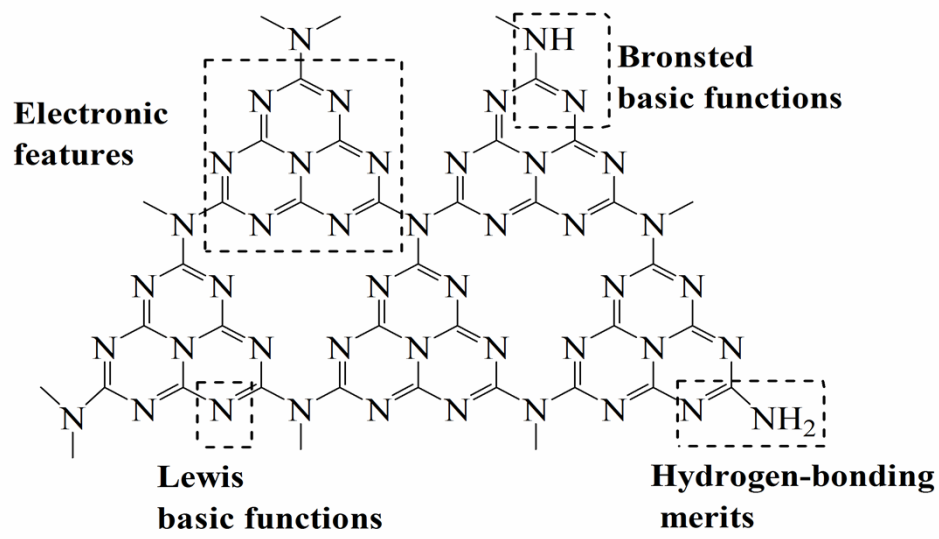

Scheme 3. Multiple surface functionalities found on sCN nanomaterials.

In view of the chemical structures of polymer containing quaternary ammonium chloride (PQACl) displayed in Scheme S1, a small quantity of Cl has been possibly introduced into the perovskite ($MAPbI_3$) during the inclusion engineering process. And their combination can evidently allow the chemical reactions during the perovskite formation, as shown below:

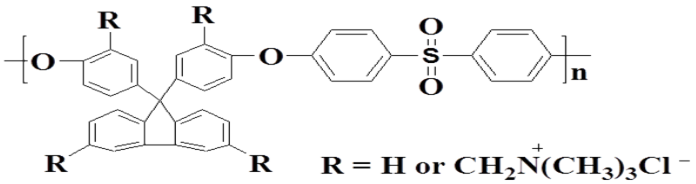

PQACl

The chemical reactions during the perovskite formation are:

$PQACl + PbI_2 + MAI \rightarrow PQAI + PbCl_2 + MACl$ (a)

$MAI + PbI_2 + PbCl_2 + MACl \rightarrow MAPbI_3\text{-}xClx + MACl$ (g) (b)

$PQAI + MACl$ (g) $\rightarrow PQACl + MAI$ (c)

As a consequence of great electronegativity of chlorine atom, iodide ions in PbI_2 and MAI may interchange with chloride ions generating $PbCl_2$ and MACl. The chloride ions in the initiated $PbCl_2$ continue to switch with the iodide ions from the perovskite precursor, leading to the formation of mixed halide perovskite film, $MAPbI_3$-xClx. Through the perovskite crystal annealing process, the PQA ions may also detain the chloride ions and therefore prohibit MACl gas expulsion, leading to disappearance of pinholes and negligible defects.

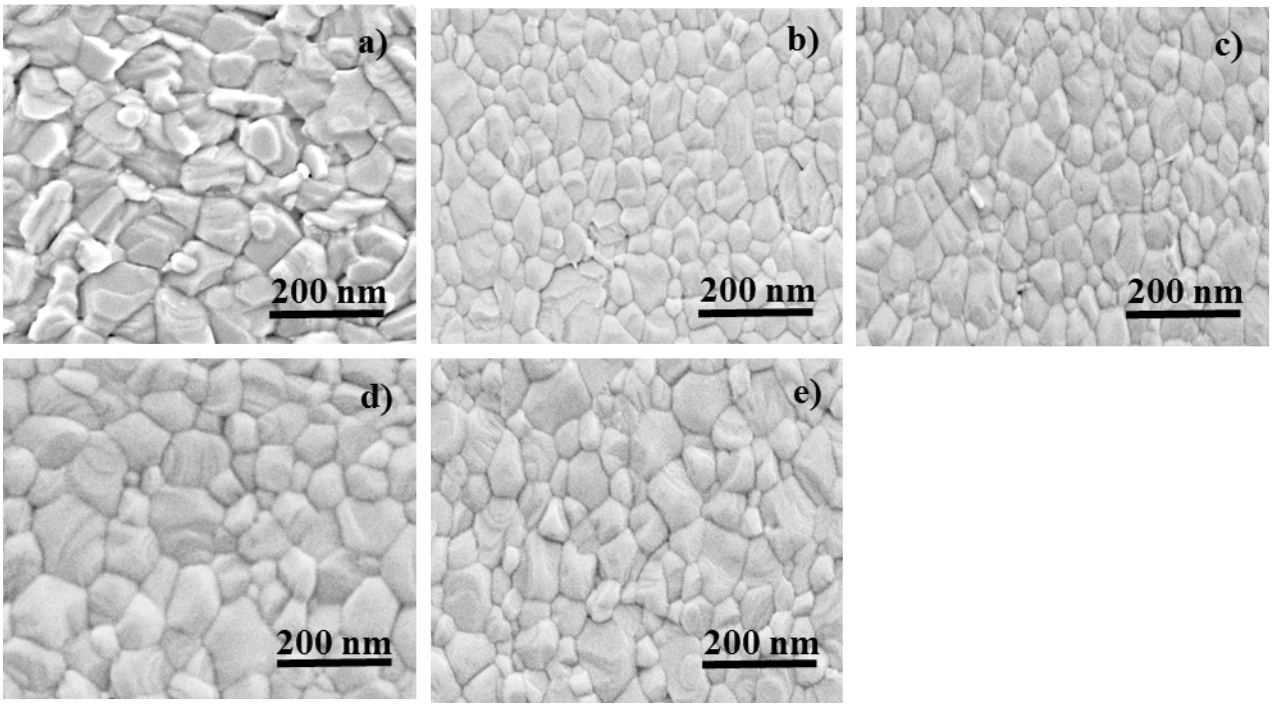

Figure S7. Top-view SEM images of a) reference and perovskite films from nanofiller materials: b) sCN1, c) sCN2, d) sCN3, and e) sCN4.

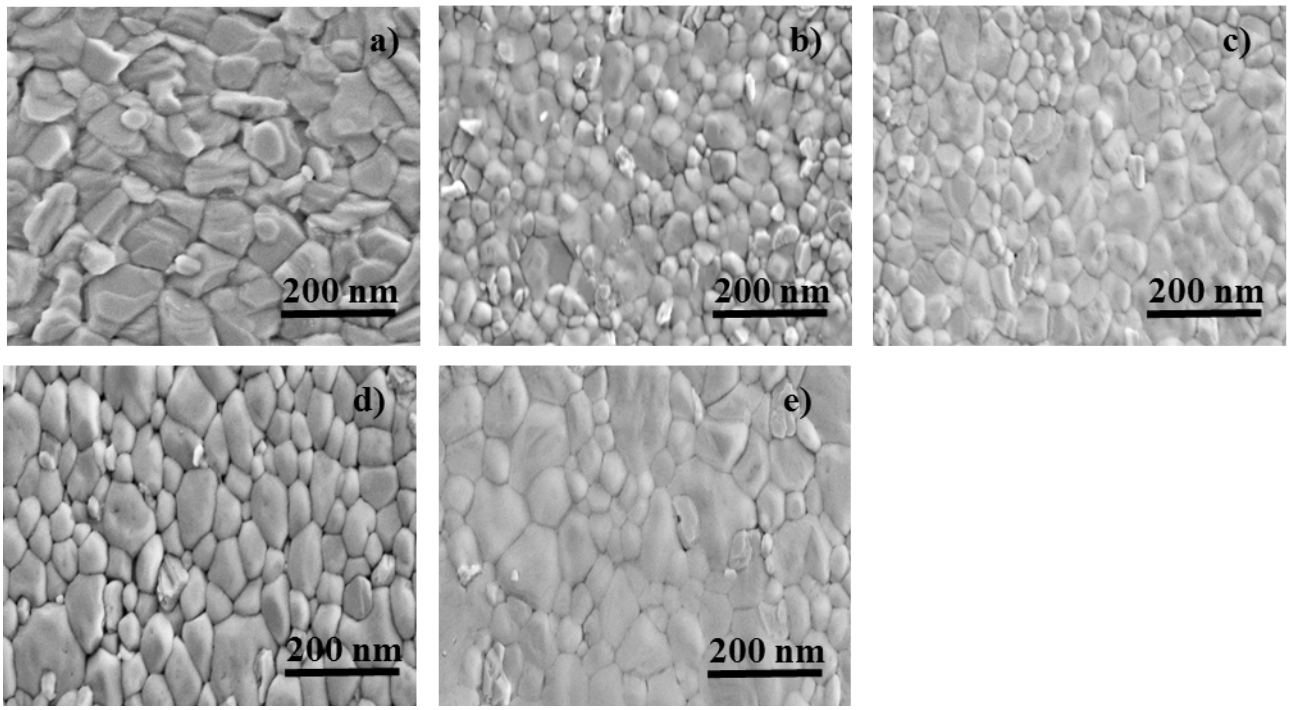

Figure S8. Top-view SEM images of a) reference and perovskite films from polymeric solution: b) PQACl1, c) PQACl2, d) PQACl3, and e) PQACl4.

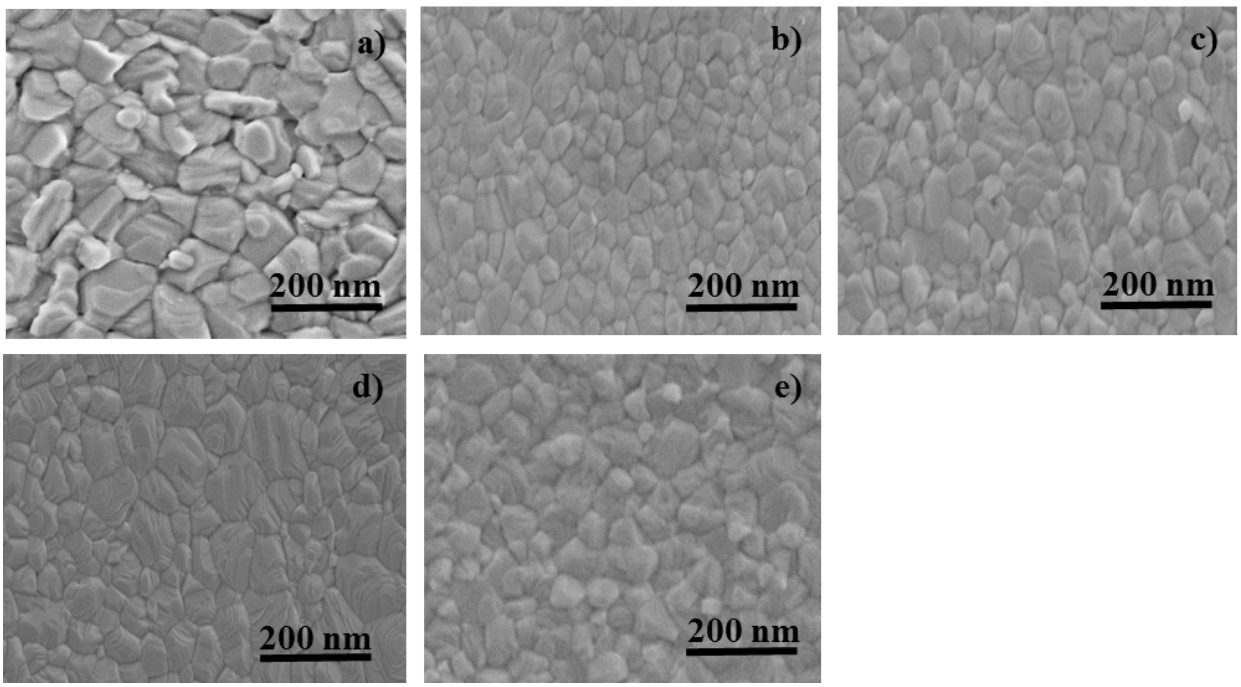

Figure S9. Top-view SEM images of a) reference and perovskite films from polymer hybrid solution: b) PQACl-CN1, c) PQACl-CN2, d) PQACl-CN3, and e) PQACl-CN4.

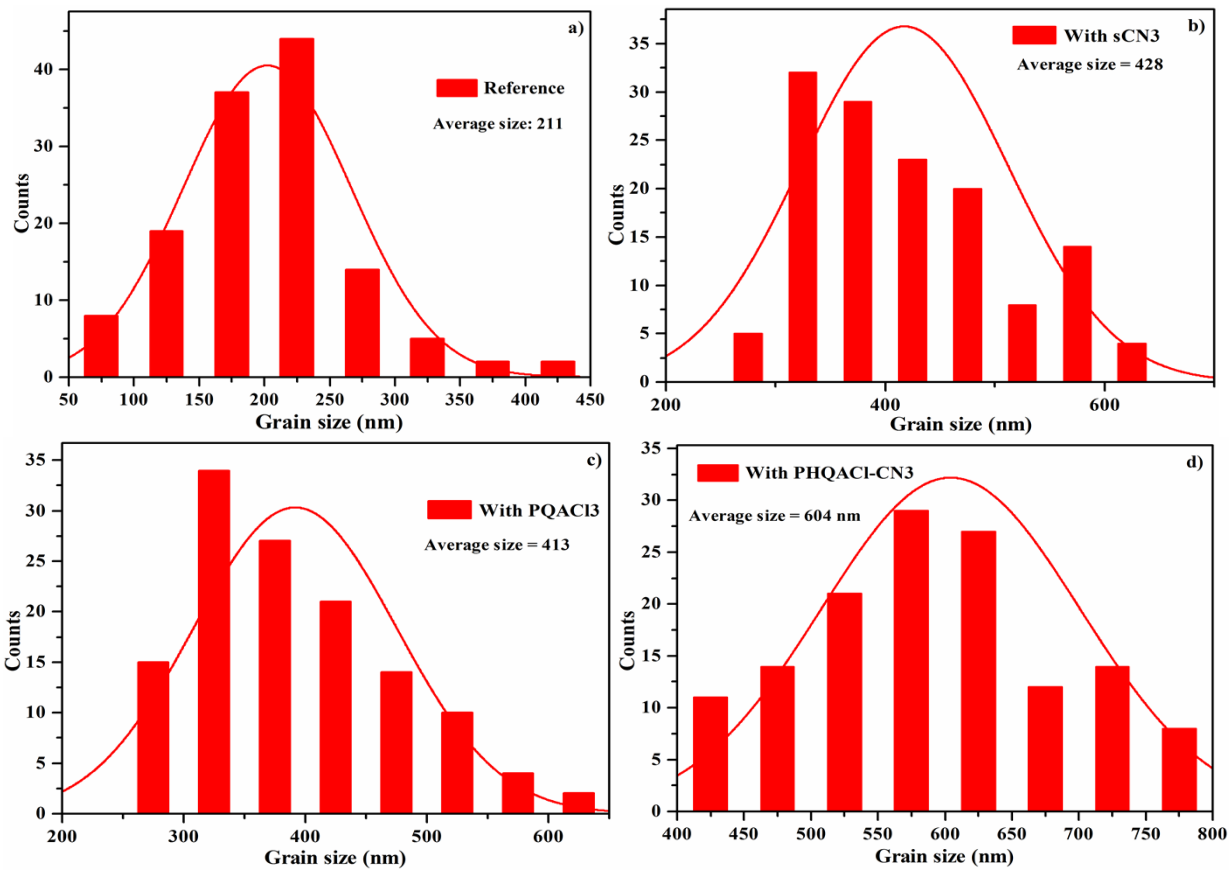

Figure S10. Histogram of grain size distributions for reference and perovskite-structured polymer films

Table XRD data

Perovskite sample	FWHM
Reference	0.1645°
With sCN3	0.1822°
With PQACl3	0.1754°
With PHQACl-CN3	0.1978°

FWHM: The full width at half maximum (FWHM)

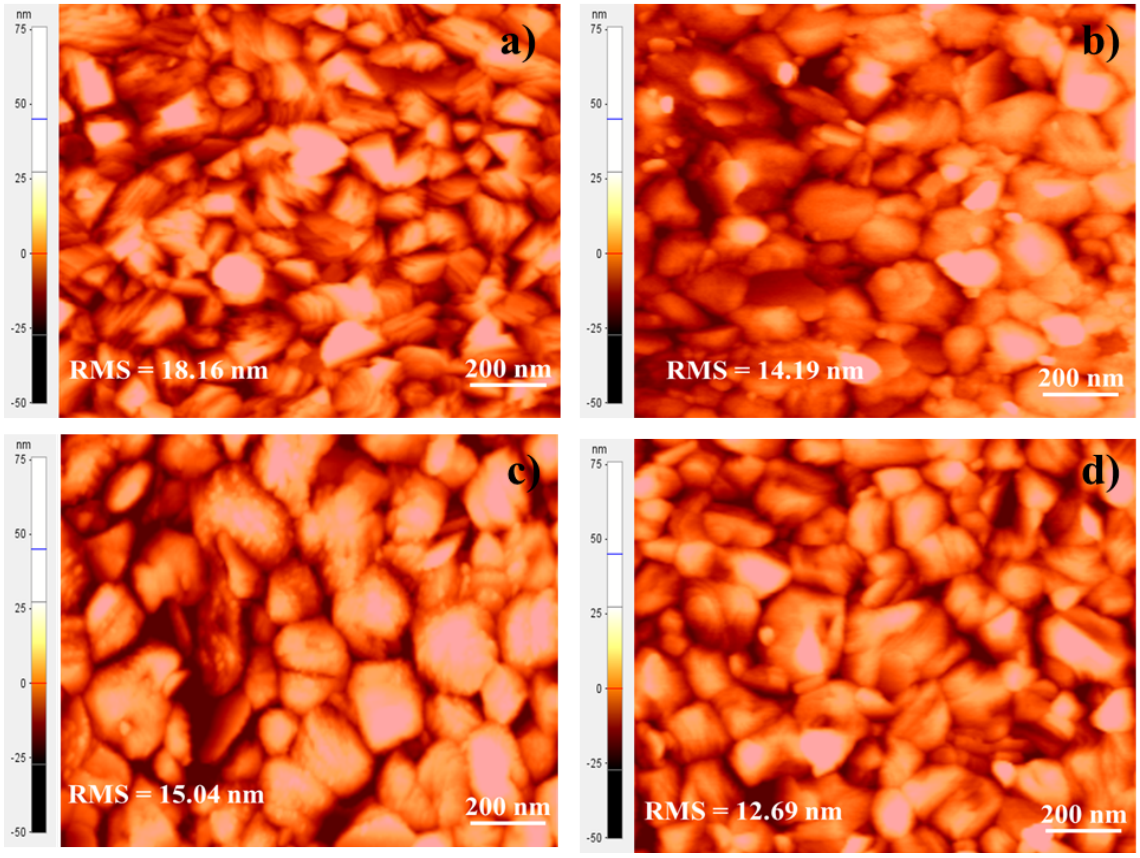

Figure S11. Analysis of the AFM images of a) Reference, b) perovskite from sCN3, c) PQACl3, and d) PQACl-CN3.

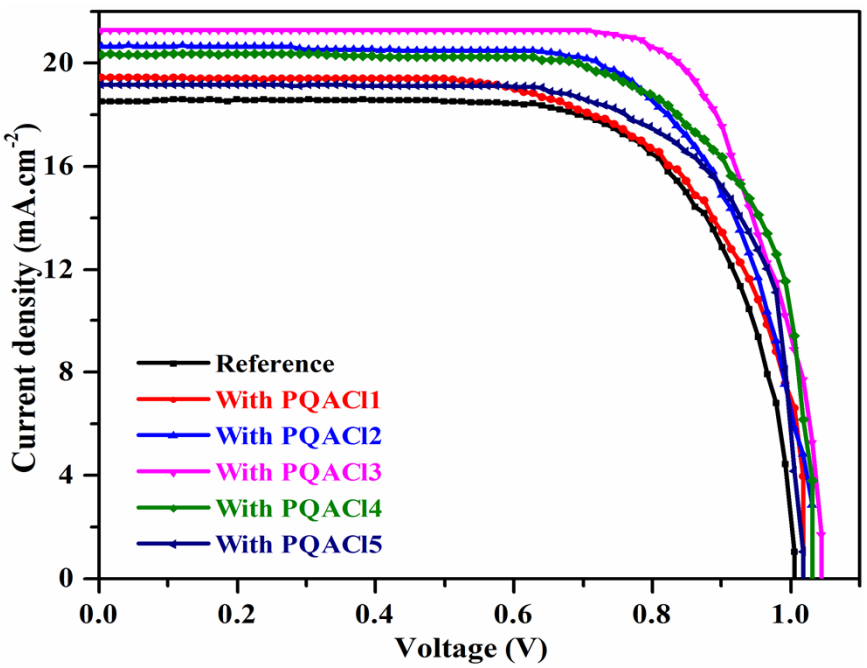

Figure S12. J-V curve from perovskite with PQACl inclusion

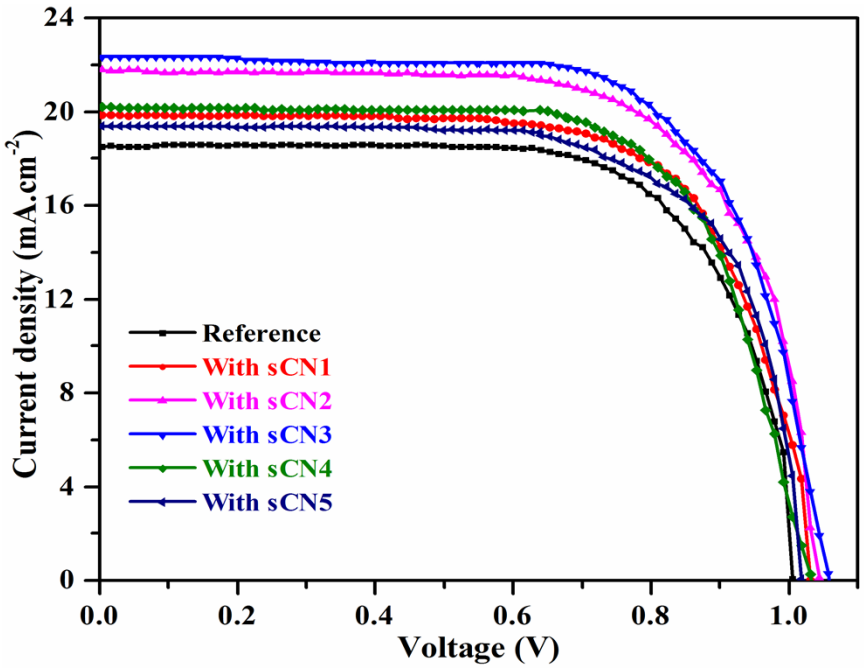

Figure S13. J-V curve from perovskite with sCN inclusion

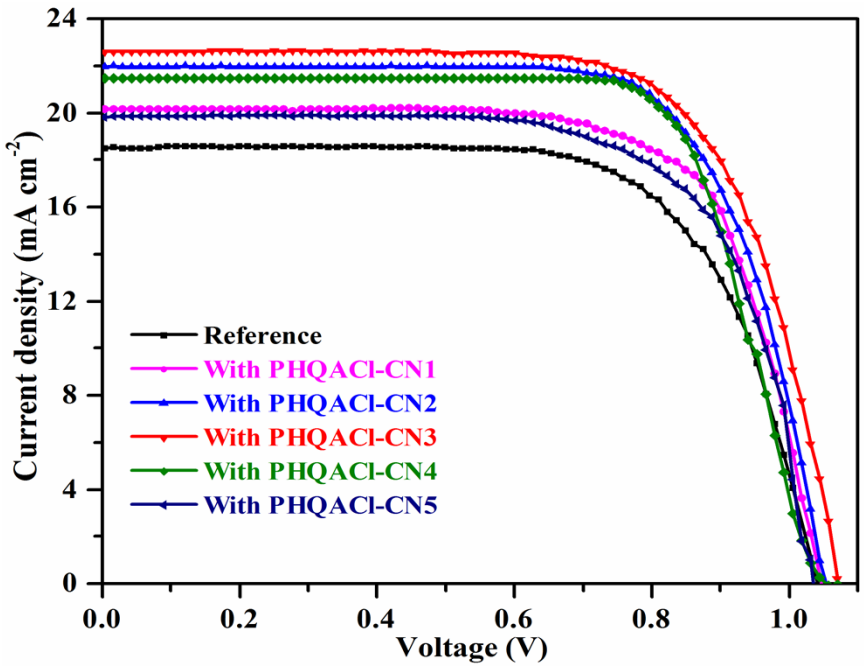

Figure S14. J-V curve from perovskite with PQACl-CN3 inclusion

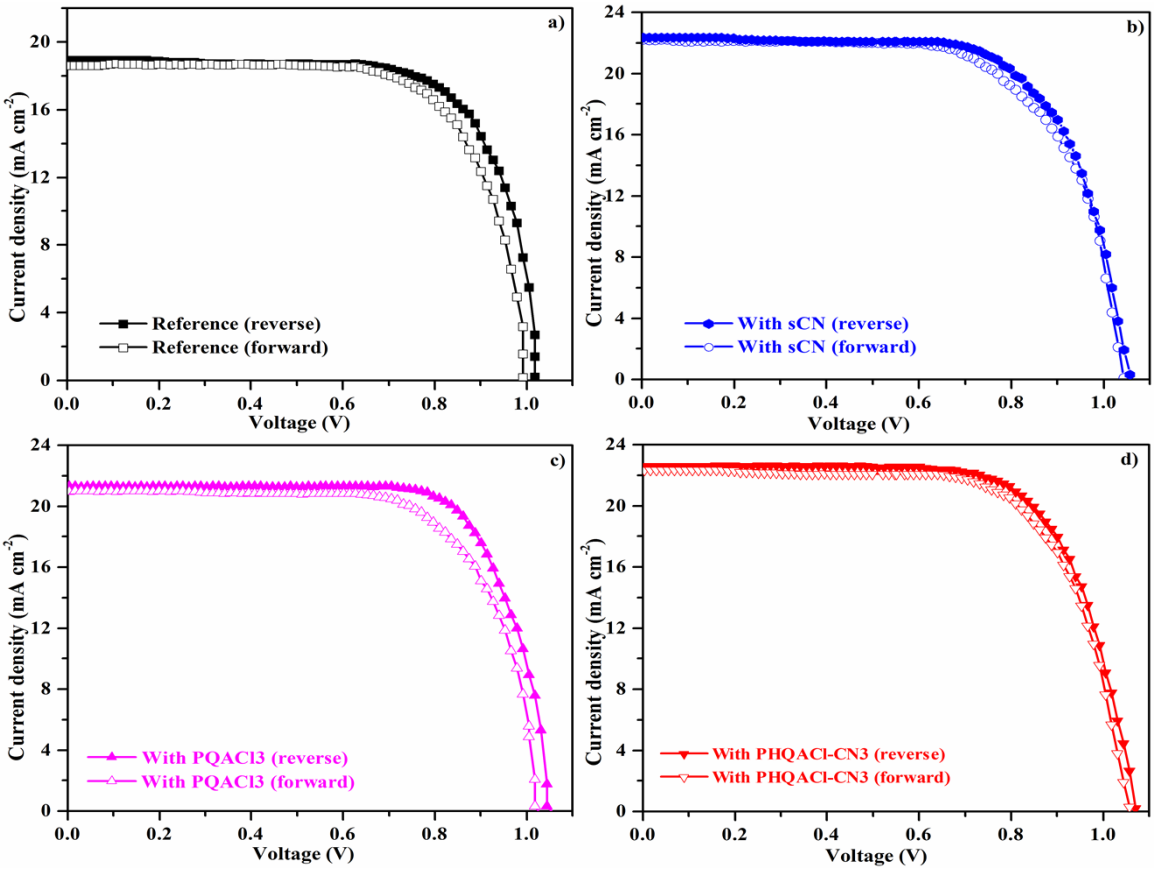

Figure S15. Comparative J-V curves from reference and perovskite with sCN3, PQACl3 and PHQACl-CN3 inclusion

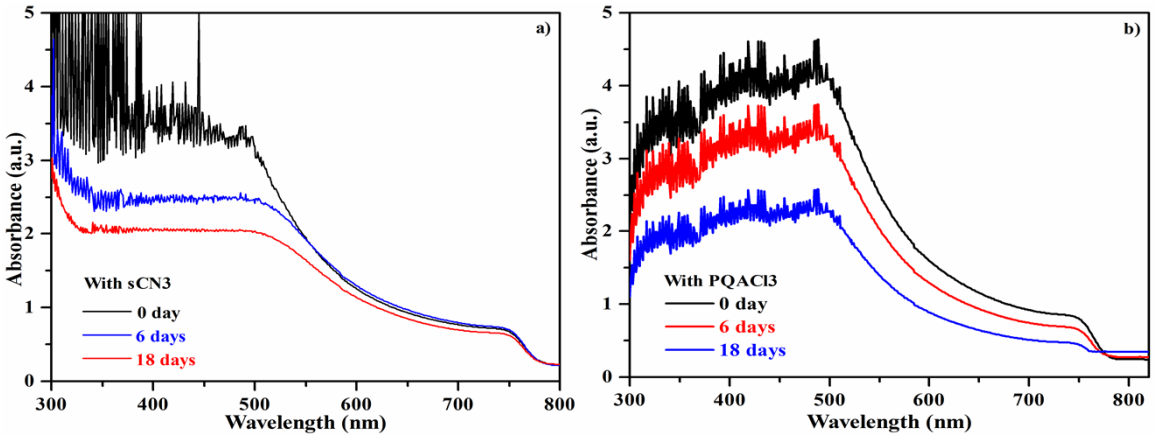

Figure S16. The normalized light absorbance of un-encapsulated perovskite films manipulated with of a) sCN3 and b) PHQACl3, tested in an ambient condition with 45-50%RH.

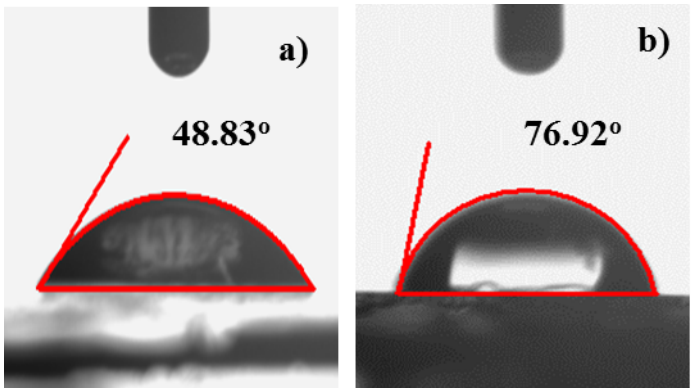

Figure S17. Water angle values of the top-performing perovskite (with PHQACl-CN3) and reference films measured under ambient temperature with 40-50 %RH after 18 days.

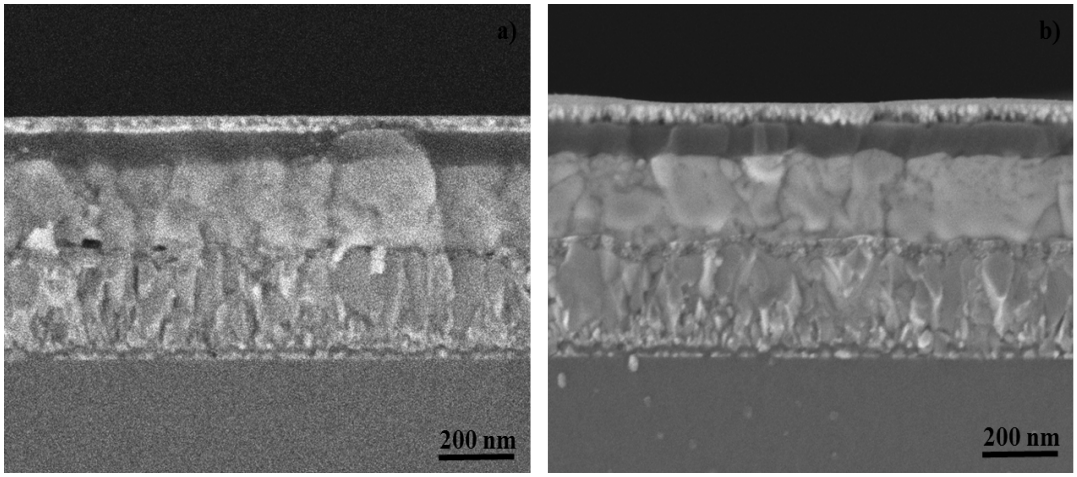

Figure S18. Cross-sectional SEM images of PSC devices from reference and PHQACl-CN3 inclusion exposed to ambient temperature with 45-50 %RH after 18 days.

Space-Charge-Limited-Current (SCLC) technique

The trap-state density voltages (V_{TFL}) in perovskite films are investigated by applying the space-charge-limited-current (SCLC) technique is to the electron transport layer (ETL)-only devices[7]. The trap-state density (Ntrap) is calcuated by the equation:

$$N_{trap} = \frac{2\varepsilon_0 \varepsilon V_{VTL}}{eL^2}$$

where ε is the relative dielectric constant of the perovskite, ε_0 is the vacuum permittivity, V_{TFL} is the trap-filled limit voltage, e is the electron charge, and L is the thickness of the perovskite.

Table S1. Solubility of the prepared polymer of quaternary ammonium chloride (PQACl)

Polymer name	**Type of solvent**			
[a]PQACl	DMF +	DMF +	DMAc +	NMP +

[a] At 6 wt%(w/v), room temperature (22-25 ^{o}C;

+: soluble

Table S2. The detailed PL parameters of the reference and delegated perovskite films.

Sample	A_1	A_2	τ_1 (ns)	τ_2 (ns)	τ_{avg} (ns)
Reference	0.67	0.20	3.2	12.8	8.0
With sCN3	0.72	0.37	7.9	20.6	14.2
With PQACl3	0.56	0.24	10.3	27.9	19.1
With PHQACl-CN3	0.62	0.30	13.6	48.7	31.1

The hysteresis index (HI) is quantified by the following equation:

$$HI = (PCE_{reverse} - PCE_{forward}) / PCE_{reverse}$$

Table S3. Detailed photovoltaic parameters of the PSCs with and without polymer materials inclusion.

Device		V_{oc} (V)	J_{sc} (mA cm^{-2})	FF	PCE (%)	HI
Reference	reverse	1.018	19.27	59.11	13.24	0.089
	forward	1.005	18.89	58.86	12.05	
With sCN3	reverse	1.057	22.34	67.85	16.88	0.021
	forward	1.044	22.18	67.68	16.51	
With PQACl3	reverse	1.044	21.29	65.43	15.46	0.032
	forward	1.031	21.03	64.26	14.97	
With PHQACl-CN3	reverse	1.07	22.62	71.27	18.21	0.017
	forward	1.07	22.55	70.18	17.89	

Table S4. The detailed parameters of electrochemical impedance spectroscopy of the champion PSCs

PSC device	Rs (Ω)	Rct (Ω)
Reference	12.19	11098
With sCN3	17.40	18457
With PQACl3	15.51	14986
With PHQACl-CN3	20.44	21230

Table S5. Comparative performance and stability data for the constructed PSCs devices.

Perovskite with	PCE	RH (%)	Stability with time	Ref.
2-pyridylthiourea	18.2	55-60	92%, 720 h	[8]
HI solution	17.2	50	-	[9]
ZnO nanoparticles	18.3	55–65	-	[10]
Thiazole	18.0	-	-	[11]
SC-PEDOT:PSS	19.1	50	83%, 336 h	[12]
4-tert-butylpyridine	16.1	10-50	80%, 240 h	[13]
PHQACl-CN	18.2	20-30	82%, 320 h	This work

References

[1] Tanaka M, Fukasawa K, Nishino E, Yamaguchi S, Yamada K, Tanaka H, et al. Anion Conductive Block Poly(arylene ether)s: Synthesis, Properties, and Application in Alkaline Fuel Cells. Journal of the American Chemical Society. 2011;133:10646-54.

[2] Ingabire PB, Pan X, Haragirimana A, Li N, Hu Z, Chen S. Improved hydroxide conductivity and performance of nanocomposite membrane derived on quaternized polymers incorporated by titanium dioxide modified graphitic carbon nitride for fuel cells. Renewable Energy. 2020;152:590-600.

[3] Aleksandrzak M, Kukulka W, Mijowska E. Graphitic carbon nitride/graphene oxide/reduced graphene oxide nanocomposites for photoluminescence and photocatalysis. Applied Surface Science. 2017;398:56-62.

[4] Yang S, Gong Y, Zhang J, Zhan L, Ma L, Fang Z, et al. Exfoliated Graphitic Carbon Nitride Nanosheets as Efficient Catalysts for Hydrogen Evolution Under Visible Light. Advanced Materials. 2013;25:2452-6.

[5] Yuan Y-J, Shen Z, Wu S, Su Y, Pei L, Ji Z, et al. Liquid exfoliation of g-C3N4 nanosheets to construct 2D-2D MoS2/g-C3N4 photocatalyst for enhanced photocatalytic H2 production activity. Applied Catalysis B: Environmental. 2019;246:120-8.

[6] Zhou Z, Wang J, Yu J, Shen Y, Li Y, Liu A, et al. Dissolution and Liquid Crystals Phase of 2D Polymeric Carbon Nitride. Journal of the American Chemical Society. 2015;137:2179-82.

[7] Shi D, Adinolfi V, Comin R, Yuan M, Alarousu E, Buin A, et al. Solar cells. Low trap-state density and long carrier diffusion in organolead trihalide perovskite single crystals. Science. 2015;347:519-22.

[8] Sun M, Zhang F, Liu H, Li X, Xiao Y, Wang S. Tuning the crystal growth of perovskite thin-films by adding the 2-pyridylthiourea additive for highly efficient and stable solar cells prepared in ambient air. Journal of Materials Chemistry A. 2017;5:13448-56.

[9] Heo JH, Song DH, Han HJ, Kim SY, Kim JH, Kim D, et al. Planar CH3NH3PbI3 Perovskite Solar Cells with Constant 17.2% Average Power Conversion Efficiency Irrespective of the Scan Rate. Advanced Materials. 2015;27:3424-30.

[10] Wang W-T, Sharma J, Chen J-W, Kao C-H, Chen S-Y, Chen C-H, et al. Nanoparticle-induced fast nucleation of pinhole-free PbI2 film for ambient-processed highly-efficient perovskite solar cell. Nano Energy. 2018;49:109-16.

[11] Zhang H, Chen H, Stoumpos CC, Ren J, Hou Q, Li X, et al. Thiazole-Induced Surface Passivation and Recrystallization of CH3NH3PbI3 Films for Perovskite Solar Cells with Ultrahigh Fill Factors. ACS Applied Materials & Interfaces. 2018;10:42436-43.

[12] Zhang P, Chen W-H, Yin X, Song L, Jiang P-C, Du P, et al. High efficiency of 19% for stable perovskite solar cells fabrication under ambient environment using “conductive polymer adhesive”. Journal of Power Sources. 2021;507:230302.

[13] Chen W-H, Qiu L, Zhuang Z, Song L, Du P, Xiong J, et al. Simple fabrication of perovskite solar cells with enhanced efficiency, stability, and flexibility under ambient air. Journal of Power Sources. 2019;442:227216.